Research Square

Preprints are preliminary reports that have not undergone peer review.
They should not be considered conclusive, used to inform clinical practice,
or referenced by the media as validated information.

Integrative epigenomic and transcriptomic profiling reveals dysregulated T cell regulatory networks in Stage 3 Type 1 diabetes

Ying Y Wong

yingying.wong@adelaide.edu.au

Adelaide University

Jessica E Harbison
Adelaide University

Daniel Hassan
Adelaide University

Batjargal Gundsambuu
Adelaide University

Christopher M Hope
Robinson Research Institute

Soon W Wong
Flinders University

Jennifer J Couper
Adelaide University

Jason A Gummow
Adelaide University

Jimmy Breen
Adelaide University

Ning Liu
Adelaide University

Stephen M Pederson
Adelaide University

Maren Kohne
German Center for Neurodegenerative Diseases, University of Bonn

Kristian Händler
German Center for Neurodegenerative Diseases, University of Bonn

Simone Picelli
Institute of Molecular and Clinical Ophthalmology Basel

Marc Beyer

German Center for Neurodegenerative Diseases, University of Bonn

Joachim Schultze

German Center for Neurodegenerative Diseases, University of Bonn

Timothy Sadlon

Adelaide University

Simon C Barry

Adelaide University

Research Article

Keywords:

Posted Date: April 7th, 2026

DOI: https://doi.org/10.21203/rs.3.rs-9142251/v1

License: This work is licensed under a Creative Commons Attribution 4.0 International License.
Read Full License

Additional Declarations: No competing interests reported.

Abstract

Aims/hypothesis.

Type 1 diabetes (T1D) is driven by destruction of the pancreatic beta cells by autoreactive T cells, which occurs as a result of failed immune tolerance. The disruptions to the molecular mechanisms that maintain this tolerance are complex, and the balance between conventional $CD4^+$ T cells (Tconv) and regulatory T cells (Treg) in T1D remain poorly defined. We hypothesised that by integrating chromatin accessibility, 3D chromatin organisation, transcriptomes and functional perturbation we can reveal the key T cell-centred networks altered in T1D.

Methods.

We performed parallel ATAC-seq and RNA-seq on sorted stimulated Tconv and Treg from children with T1D and age-matched autoantibody-negative controls. We mapped differentially accessible (DA) regions to putative target genes in human Treg and activated $CD4^+$ T cells using Hi-C and asked whether 3D contacts assigned enhancers to distal genes not captured by nearest-gene annotation. To interrogate rare T cell subsets and age effects, we analysed single-cell RNA-seq (scRNA-seq) data from peripheral blood mononuclear cells (PBMCs) of adults with T1D and controls. Finally, we used CRISPR–Cas13d to perform multiplex knockdown of 7 candidate transcription factors (TFs) from a TNFα/NF-κB–linked module (FOS, FOSL1, FOSL2, MAFF, EGR1, EGR2 and NR4A3) in primary human Treg, followed by RNA-seq to functionally test the impacts.

Results.

Hundreds of differentially accessible regions and expressed genes were detected in paediatric Treg and Tconv cells in T1D, with changes enriched for TNFα signalling via NF-κB, interferon responses and IL-2/STAT signalling. TF footprinting highlighted altered occupancy at AP-1 motifs and other immune regulators, consistent with subtle rewiring of regulatory circuits. Integration with T cell Hi-C revealed that a large fraction of T1D-altered enhancers contacts genes other than the nearest transcription start site and uncovered new altered enhancer-gene pairs. Cas13d-mediated 7-TF knockdown induced transcriptional changes strongly overlapping those seen in paediatric T1D Treg.

Conclusions.

By combining paediatric case–control T-cell ATAC-seq and RNA-seq with T cell Hi-C, adult single-cell transcriptomes and CRISPR–Cas13d perturbation, we describe a multi-layered, Treg-centred network in T1D. This integrative framework provides a blueprint for moving from non-coding association signals to

mechanistic models of T-cell dysregulation in T1D and suggests candidate pathways for therapeutic intervention.

Introduction

Type 1 diabetes (T1D) is a chronic autoimmune condition characterised by T cell–mediated destruction of pancreatic β-cells, and multiple immune cell populations contribute to disease pathogenesis. $CD4^+$ T cells play critical roles in both initiating and sustaining islet autoimmunity[1–3], and in health, a fine balance between conventional T cells (Tconv) and regulatory T cells (Treg) is critical for maintaining self-tolerance. $CD4^+$ T cells comprise multiple maturation states and subpopulations, including naive, memory and effector/helper pools that coordinate immune activation. $FOXP3^+$ Treg restrain these responses to prevent autoimmunity, and defects in Treg number, stability or suppressive function [4–6], together with dysregulated Tconv responses, contribute to the breakdown of immune tolerance to β-cell antigens observed in individuals living with T1D. However, the molecular mechanisms that underpin these functional abnormalities in T cells, particularly in children close to disease onset, remain incompletely understood. Clinically, T1D is a multi-stage autoimmune disease, starting with the appearance of islet autoantibodies (Stage 1) and progressing through a preclinical phase marked by β-cell destruction, declining glycaemic control (Stage 2) and eventual insulin dependency (Stage 3). Defining the mechanisms that characterize T-cell dysfunction early may highlight pathways that arise at diagnosis for therapeutic intervention.

T1D has a genetic component which interacts with environmental changes that trigger progression, and genome-wide association studies have identified more than 100 risk loci for T1D [7], the majority of which sit in non-coding regions of the genome [8–11]. These variants are mostly found in regulatory elements such as enhancers and promoters active in immune cells, including $CD4^+$ Tconv cells and Treg, suggesting that perturbation of gene regulation is a major mechanism through which genetic risk is exerted. Chromatin accessibility and histone modification studies further indicate that T1D risk variants are concentrated in enhancers responsive to T cell activation. Yet, the precise linkage between disease-associated regulatory elements and their target genes remains poorly resolved, especially in paediatric T cell subsets. In particular, although Hi-C and related technologies have provided 3D chromatin maps for human T cells [12–14], there is a lack of systematic frameworks that connect T1D-associated changes in enhancer activity to their three-dimensional (3D) contacts and to the transcriptional programs they control.

Recent omics studies have begun to address these questions but remain incomplete. Bulk transcriptomic profiling and eQTL (expression quantitative trait locus) analyses have been performed predominantly in PBMCs or bulk T cells [15–17], which limits resolution of cell type–specific effects, particularly in rare Treg. More recently, joint profiling of chromatin accessibility and gene expression in disease-relevant immune tissues has begun to characterize regulatory changes directly in individuals with or at risk of T1D [18]. Nevertheless, most available T1D immunogenomic studies [18–25] still profile bulk/unfractionated $CD4^+$ T cells at a single modality, and relatively few integrate chromatin accessibility

and gene expression from the same individuals, limiting the ability to link regulatory activity to downstream transcriptional programmes. In addition, most datasets are derived from resting cells, despite growing evidence from eQTL studies that disease-relevant regulatory effects are frequently amplified or only detectable following T-cell activation, where they show increased colocalization with autoimmune risk variants [26, 27]. Paediatric T1D also remains underrepresented in these analyses[19, 20]. Emerging data indicate that immune cell composition [28, 29], activation thresholds [30, 31] and transcriptional responses [32] differ between children and adults, supporting the hypothesis that regulatory mechanisms altered in paediatric T1D may not be fully captured by adult studies. Furthermore, 3D chromatin conformation data in T cells has largely been derived from healthy adult cells and rarely in the T1D context. Finally, functional validation of genetic variants, candidate TFs or pathways using CRISPR-based perturbation in human primary Treg remains limited.

To address these knowledge gaps, here we integrate paediatric T1D Tconv/Treg chromatin accessibility, matched gene expression, adult T cell Hi-C, T1D single-cell transcriptomes and CRISPR–Cas13d perturbation to derive and functionally test a Treg-centric regulatory network in the context of T1D. Specifically, we set out to **(1)** map T1D-associated changes in chromatin accessibility and gene expression in paediatric Tconv and Treg under stimulation, using parallel ATAC-seq and RNA-seq to link regulatory elements to transcriptional output; **(2)** use T cell Hi-C to connect altered enhancers to their likely target genes and assess whether these genes are dysregulated in T1D, thereby providing a 3D, cell type–specific framework for interpreting non-coding regulatory changes in Tconv and Treg, and **(3)** identify and functionally validate a TF network altered in T1D Treg using CRISPR–Cas13d knockdown in primary Treg cells. Together, this multi-omic approach combined with targeted perturbation moves us from correlation to mechanism of action, enabling understanding of altered enhancer–promoter connectivity and regulatory networks contributing to loss of immune tolerance in T1D.

Results

Characteristics of the paediatric cohort and overview of multi-omic profiling. We first accessed cryopreserved peripheral blood mononuclear cell (PBMC) samples from the Australian Type 1 Diabetes and the Gut (TIGs) cohort [33, 34], a prospective study of youth with islet autoimmunity (IA) or recent-onset type 1 diabetes, and age-matched autoantibody-negative controls. From this biobank, we selected a subset of 12 children with recent-onset T1D for whom sufficient PBMC material was available for isolation of $CD4^+$ T cells (Fig. 1A; **Table 1**). The case and control groups were similar in sex distribution (58.3% vs 66.7% male, $P > 0.9999$) and PBMC viability (89.0 ± 2.7% vs 88.3 ± 3.5%, $P = 0.350$), and there was no statistically significant difference in age at sampling (9.8 ± 2.0 vs 12.3 ± 4.0 years, $P = 0.096$; **Table 1**). There were no significant differences between cases and controls for either viability or PBMC recovery (**Supplementary Fig. 1B**). PBMCs were sorted into conventional T (Tconv) and regulatory T (Treg) subsets for ATAC-seq and RNA-seq after polyclonal stimulation of CD3/CD28 (Fig. 1A; **Supplementary Fig. 1A**).

T1D is associated with widespread chromatin and transcriptional changes in paediatric T cells. We next asked how T1D status affects regulatory landscapes and gene expression in paediatric $CD4^+$ T cells. Immune transcriptomic alterations [11, 13, 22] have not yet been explored in paediatric cohorts using matched ATAC-seq and RNA-seq from stimulated T cells. Differential accessibility (DA) analysis was restricted to T cell enhancer-annotated peaks [9] to focus on changes at distal regulatory elements, which are enriched for autoimmune GWAS variants and exhibit strong activity following T-cell stimulation. Using matched ATAC-seq and RNA-seq from Treg and Tconv cells, we detected hundreds of differentially accessible (DA) peaks and differentially expressed (DE) genes in children with T1D and controls (Fig. 1B–D). In Treg, 386 loci showed increased and 289 decreased accessibility in T1D, whereas in Tconv cells 168 loci were more accessible and 886 less accessible in T1D (Fig. 1B-C). At the transcript level, 139 genes were upregulated and 213 downregulated in Treg, and 125 genes were upregulated and 212 downregulated in Tconv cells (Fig. 1B, D; FDR < 0.05). This supports that T1D perturbations are polygenic and modest magnitude in size [22, 23]. Several DE genes annotated in previous T1D studies [19, 22, 23, 35], or reported as FOXP3 targets [36] were among the significantly altered transcripts, including *FOSL2*, *MAF*, *TNF* and *CCR5*, highlighting that our profiling validates established disease and Treg biology markers while also uncovering additional candidates and pathways.

Disease-associated changes converge on immune regulatory pathways. To understand the biological programmes affected by these chromatin and transcriptional changes, we performed pathway and gene set enrichment analyses (GSEA) on both ATAC-seq and RNA-seq datasets (Fig. 2). KEGG and GSEA Hallmark analysis of differentially accessible (DA) peaks in Treg and Tconv cells showed significant enrichment for immune signalling and activation pathways (Fig. 2A, B). In particular, DA regions in both subsets were enriched for TNFα signalling via NF-κB, interferon-γ response and IL-2/STAT signalling, indicating that the enhancer regions gaining or losing accessibility in T1D regulate inflammatory and cytokine pathways in both cell types. Some of these pathways have been reported altered in T1D [17, 19–21]. KEGG network representations revealed that many DA regions in both Treg and Tconv cells cluster in interconnected gene sets rather than isolated loci, reinforcing coordinated modulation of immune regulatory modules in T1D.

At the transcriptional level, GSEA revealed broadly overlapping pathway alterations in Treg and Tconv cells from T1D compared to healthy controls (Fig. 2C, D). Notably, the majority of significant pathways were downregulated in both subsets (11/13 in Treg and all 11 in Tconv), indicating a shared attenuation of core immune programmes. These included ligand–receptor interactions and inflammatory pathways such as TNFα signalling via NF-κB, IL-2/STAT signalling, hypoxia. In addition to this overlap, subset-specific features were seen. In Treg, two upregulated pathways - E2F targets and G2M checkpoint (Fig. 2D) were linked to cell-cycle progression, suggesting altered activation dynamics. Treg also showed alterations in stress-response programmes, including unfolded protein response and UV response. In contrast, Tconv cells showed signatures consistent with metabolic rewiring, including reduced glycolysis. Together, these findings suggest that transcriptional changes collectively impact immune signalling, activation control and metabolic regulation relevant to T1D pathogenesis. The enrichment of

TNF-α/NF-κB signalling, interferon responses and cytokine-mediated pathways in our ATAC-seq and RNA-seq analyses points to a broad disturbance of inflammatory wiring in T cells in T1D.

Altered transcription factor footprints indicates rewiring of regulatory circuits. Genetic and epigenomic studies indicate many non-HLA T1D genetic variants map to non-coding, cell-state-specific regulatory elements rather than producing protein-coding changes [8, 10, 11]. This suggests that risk is likely mediated through disruption of cis-regulatory element function, including altered TF activity, leading to multiple downstream shifts in gene expression. We next examined TF "footprints" within DA peaks (Fig. 3). Using footprint analysis on pooled ATAC-seq data from the 12 matched case–control pairs, we identified multiple TF motifs whose activity differed significantly between T1D and control in Treg and Tconv cells (Fig. 3A). In Treg, the most significantly altered motifs included ZBTB7C, GMEB1 and E2F1, which are consistent with the enrichment of E2F target and G2M checkpoint pathways seen at the transcriptomic level. More broadly, accessibility was increased at motifs for several FOX/Runx-like factors and decreased at a broad set of AP-1 dimers (FOS, FOSL1/FOSL2:JUNB and related motifs). In Tconv, the strongest accessibility changes were observed at motifs for NRF1, GMEB2, SMAD3 and HES2. Increased accessibility was seen at multiple EGR family motifs and reduced accessibility at AP-1-related and cell-cycle–associated motifs (FOSL2:JUNB, MYBL2). Notably, AP-1 family motifs such as FOS/FOSL2::JUNB are down in both Treg and Tconv cells, indicating a shared attenuation of AP-1–driven regulation in both subsets. Representative motif-centred profiles around selected TF binding sites show comparable accessibility and depth at the predicted engagement sites between T1D and control, but modest shifts in accessibility in the flanking regions (Fig. 3B), suggesting that T1D may fine-tune the local chromatin landscape around TF binding sites rather than strongly altering occupancy at the core motif. Several of the TFs whose motifs showed altered signals also showed differential expression in our RNA-seq data that are consistent with the direction in the change in accessibility (Fig. 3C). Together, these results support a model in which T1D is associated with subtle rewiring of TF-centred regulation in T cells, in line with focussed coordinated effects seen at the level of chromatin accessibility and gene expression (Fig. 1). Genomic regions showing differential TF footprints between T1D and control were strongly enriched for immune pathways (Fig. 3D). In Treg, footprint-altered regions mapped to gene sets involved in lymphocyte differentiation and activation, Toll-like receptor signalling, TNFα–NF-κB signalling, IL-2–STAT5 signalling and regulation of apoptotic and defence responses, pointing to broad perturbation of inflammatory priming and survival programmes. In Tconv cells, the same analysis highlighted pathways of T-cell activation and differentiation, leukocyte chemotaxis and migration. The pathways enriched in altered TF footprints mirrored those identified from our bulk ATAC-seq and RNA-seq analyses (Fig. 2). For instance, altered TF footprints in Treg cells were enriched for TNFα signalling via NF-κB, IL-2–STAT5 signalling, signalling receptor pathways and lymphocyte activation, consistent with the pathways identified by RNA-seq (Figs. 2 and 3D). In Tconv cells, altered footprints mapped to pathways controlling T-cell activation, leukocyte chemotaxis/migration and chemokine receptor activity, again overlapping the activation and inflammatory terms seen in Fig. 2. This concordance suggests a coherent regulatory model in which altered TF binding is coupled to changes in chromatin accessibility at

enhancer elements, contributing to downstream transcriptional changes, with TNFα/NF-κB linked signalling and AP-1 family factors standing out as key axes of perturbation in T cells.

Network-level view of altered Treg and Tconv transcriptional programmes. To move beyond gene set enrichment and study the structural organization of dysregulated genes, we constructed interaction networks of RNA-seq DE genes in Treg and Tconv cells and overlaid GO enrichments (Fig. 4A). In Treg, DE genes formed a tightly connected module linking “regulation of gene expression” and “cytokine-mediated signalling”, centred on TF FOS, FOSL1, FOSL2, EGR1 and NR4A3 and cell–surface/secreted molecules such as CD48, ICAM1, ITGA4, CCL3/4 and IL4/5/16. This cluster points to coordinated remodelling of AP-1/EGR-driven transcriptional programmes and downstream cytokine signalling in Treg. Additional, smaller Treg clusters involved integral membrane components and G-protein–coupled receptor (GPCR) signalling, suggesting further tuning of receptor-proximal pathways and consistent with prior evidence implicating GPCR signalling CXCL10–CXCR3 axis in T-cell recruitment during early T1D [37]. In Tconv cells, the DE-gene network highlighted a distinct but related landscape (Fig. 4A, right), for instance, a module “cellular response to stimulus” containing TNF, IL2, CCR5, CCL3/4/4L1, RORC and MAF, consistent with altered inflammatory and Th1/Th17-related programmes [38, 39]. Surrounding clusters involved chemotaxis and voltage-gated potassium channel activity. The presence of MAF in this Tconv module, alongside FOS/AP-1 family members and TNF in the broader dataset, reinforces the idea that a common set of transcriptional regulators and cytokine axes is being tuned across both Treg and Tconv compartments.

We then compared expression profiles between Treg and Tconv cells to determine if there were changes in the magnitude of responses between disease and healthy control. Plotting $\log_2$ fold-change (Treg vs Tconv DGE) in T1D and control (Fig. 4B) showed the expected strong expression of classical Treg signature genes (e.g. *FOXP3*, *TIGIT*, *CTLA4*). However, a subset of Treg signature genes (e.g. *CEACAM4*, *CXCR6* and *TLR5*) displayed an increased Treg/Tconv differential in T1D (shifted above the diagonal), which could indicate selective reinforcement or reprogramming of specific activation features. Additional genes (e.g. *NELL2* and *MCOLN2*) showed subtle differential degrees of reduction between subsets, consistent with heterogeneous reshaping of Treg/Tconv transcriptional boundaries. When we examined $\log_2$ fold-change (T1D vs healthy) separately in Treg and Tconv cells (Fig. 4C), a subset of transcripts showed clear concordant changes in both cell types. Of the 38 genes commonly differentially expressed in both Treg and Tconv cells, 35 (92.1%) showed concordant directionality (**Table S1**). Genes such as *EFNA1*, *THNSL2* and *TRAV1-1* were upregulated in T1D in both Treg and Tconv cells (top-right quadrant), whereas survival/apoptosis-associated regulation [40] and effector-tolerance control genes including *BNIPL*, *MAF*, *MAFF* and *CCL4* were downregulated in both cell types (bottom-left quadrant). Notably, *TRAV1-1* encodes a TCRα variable region that has been implicated in pancreatic islet–reactive clonotypes in T1D[41]. Together, these findings reinforce that early insulin-dependent T1D is characterized by coordinated and largely subtle shifts in gene expression affecting activation, regulation and survival pathways in T cells.

Hi-C-guided enhancer–gene mapping links distal regulatory changes to T1D effector genes. To ask how much of the T1D-associated transcriptional change can be explained simply by local chromatin accessibility, we linearly annotated DA peaks to their nearest gene and compared $\log_2$ fold-changes (T1D vs control) from ATAC-seq and RNA-seq (Fig. 5A). In Treg cells, most genes clustered tightly around the origin, and a relatively small set showed concordant differential accessibility and expression (red points). Examples include *FOSL2*, *FURIN*, *DAPK1*, *ZNF257* and *AMZ1* which showed reduced accessibility accompanied by modest decreases in expression. Overall, the global correlation between ATAC and RNA was weak, suggesting that many Treg expression changes are not captured by nearest-peak annotation alone. In Tconv cells, we observed a larger number of genes that were both DA and DE, including inflammatory and signalling genes such as *CCR5*, *CCL3/4*, *IFNG*, *MAF*, *MAFF*, *EPAS1*, *ADAM19* and *LGALS3*.

In $CD4^+$ T cells long-range enhancer–promoter interactions are common and many T1D risk loci fall in non-coding, distal regulatory enhancers rather than in gene bodies [8–10] therefore assigning altered enhancers to target genes based solely on linear genomic distance is unlikely to capture many of these long-range interactions. This motivated us to use T cell Hi-C maps to re-assign T1D-altered enhancers to genes they contact in 3D space, rather than simply to the nearest gene (Fig. 5). We overlaid our paediatric Treg DA peaks (T1D vs control) with Hi-C maps from human Treg cells generated by Liu, Sadlon [13]. This dataset contains 344,462 significant interactions (minCount ≥ 5); 1,671 of these (~ 0.5%) intersected our DA peaks, indicating a small subset of Treg contacts involve enhancers with altered accessibility in paediatric T1D (**Table S2**). We then asked whether 3D contacts would change how these DA enhancers are assigned to putative target genes. Integrating Treg Hi-C with our ATAC-seq and RNA-seq data, we identified 21 Hi-C interactions that linked DA peaks to target genes that were also significantly differentially expressed in our paediatric Treg RNA-seq. Accounting for DA peaks overlapping Hi-C loops contacting multiple sites within the same target gene, 8 DE genes (*FOSL2*, *EFNA1*, *TGFA*, *IL4*, *ICAM1*, *CD48*, *LY9* and *PRSS16*) were identified in this analysis (**Table S2**). Notably, only one of these genes (*FOSL2*) was recovered by nearest-TSS annotation, whereas Hi-C–guided mapping revealed seven additional DA peak - DE gene interactions. Most of these genes are strongly associated with TNF-α via NF-κB signalling and inflammatory response (Fig. 5C; left), indicating new transcriptional regulation pathways linked to the aberrant expression of these pathways in T1D. In Tconv cells, we overlaid our paediatric Tconv DA peaks with promoter-capture Hi-C (pcHi-C) maps generated from activated total human $CD4^+$ T cells [12]. This dataset contains 221,188 significant interactions (CHiCAGO score ≥ 5), of which 4,151 intersected our Tconv DA peaks (**Table S3**). Integrating these DA–Hi-C pairs with Tconv RNA-seq revealed 2,257 interactions where the Hi-C–contacted gene was also differentially expressed in T1D, and 2,215 had a different Hi-C-assigned gene compared to linear assignment. These 2,257 interactions corresponded to 150 unique DE genes, only 13 of which were also recovered by linear annotation, meaning that 137 genes (~91%) were revealed only through 3D mapping. This Hi-C–derived set includes canonical cytokines and receptors such as *TNF*, *TNFRSF12A*, *IL10RB*, *IL2*, *IL17F* and the TF *MAF*. The gene set is linked with pathways such as glycolysis, TNF-α signalling via NF-κB, hypoxia and IL-6/JAK/STAT3 signalling (Fig. 5C), which have been reported to play a role in T1D [42–44]. For example,

at the *MAF* locus (**Supplementary Fig. 2)**, an upstream distal enhancer shows reduced accessibility in T1D Tconv cells and overlaps differential TF footprints. Although nearest-gene annotation would assign this element to *WWOX*, promoter capture Hi-C data from activated CD4⁺ T cells reveal long-range contacts with the *MAF* promoter, which is also downregulated in T1D. This shows how integrating Hi-C with ATAC- and RNA-seq may reassign enhancer changes from nearby genes to their distant regulatory targets.

Adult single-cell PBMC tanscriptomics reference confirms cross-modality and cross-age signatures. To test whether the transcriptional patterns observed in our paediatric bulk data are reflected in independent adult datasets at single-cell resolution, we analysed raw single-cell RNA-seq data provided by Parse Biosciences generated from 22 PBMC samples, comprising 12 donors with T1D and 10 non-diabetic controls (Fig. 6). T1D donors were older than controls (49.8 ± 4.8 vs 33.4 ± 9.4 years, Welch's *t* test $P \approx 0.007$), whereas the sex distribution was similar between groups (50% T1D male vs 60% control male, Fisher's exact test $P \approx 0.64$) (**Table S4**). Cell-type annotation recovered the expected diversity of PBMC populations, including naïve and memory CD4⁺ and CD8⁺ T cells, Treg, proliferating T cells, NK cells, B cells, plasma cells, dendritic cells, CD14⁺ and CD16⁺ monocytes and haematopoietic stem/progenitor cells (Fig. 6A, B). The overall proportions of major cell types were broadly similar between T1D and control, consistent with prior single-cell studies reporting minimal compositional differences in T1D [20]. We then performed subclustering on CD4⁺ T cell clusters which resolved five transcriptionally distinct CD4⁺ states corresponding to naïve, memory, proliferating, Treg and a transitional CD4 populations.

At finer granularity, we identified a transitional CD4⁺ cluster positioned between naïve CD4⁺ and Treg cells and clearly separated from the memory compartment, consistent with an intermediate or "bridge" state closer to naïve/Treg-like phenotypes than to fully differentiated memory cells. This cluster was reduced in T1D and characterized by lower expression of *MAFF*, *RORC* and additional transcripts including *TNF*, *BNIPL*, *PRSS23* and *ZNF90* (Fig. 6B,C; **Supplementary Fig. 3**). Consistently, Eugster, Lorenc [25] reported reduced *RORC* expression in a transitional antigen-specific CD4⁺ T-cell cluster in recent-onset T1D compared with controls. To determine whether the redistribution of cells reflected genuine transcriptional progression, we performed pseudotime analysis using Monocle3 (**Supplementary Fig. 4**). While memory and transitional CD4⁺ clusters did not show significant pseudotime shifts between T1D and controls, these subsets contained fewer cells, which may limit sensitivity to detect subtle trajectory difference. Naive CD4⁺, Treg and proliferating T-cell clusters showed significant differences, which may suggest selective redistribution along transcriptional trajectories in T1D rather than global alterations of CD4⁺ compartments. To place these changes in a pathway context, we performed GSEA enrichment on T1D vs control within each adult CD4⁺ subset (Fig. 6D). Across all four subsets we observed coherent enrichment of interferon-α and interferon-γ response and depletion of TNFα signalling via NF-κB. This pattern of pathway perturbation was highly similar between subsets and closely mirrored the enrichments seen in our paediatric bulk ATAC-seq/RNA-seq, including downregulation of TNFα signalling via NF-κB, glycolysis and DNA repair pathways (Fig. 2). Together, these cross-cohort and cross-modality

patterns support the idea that shared inflammatory signalling and cellular stress programs are reproducibly perturbed in $CD4^+$ T cells in T1D.

CRISPR–Cas13d perturbation of a seven-TF module in human Treg recapitulates T1D signatures. Across our datasets, TNFα signalling via NF-κB emerged as one of the most strongly downregulated pathways in Treg cells from children with T1D. It was also consistently found to be altered in paediatric Tconv cells (Fig. 2C), integrative 3D enhancer–gene mapping (Fig. 5C) and in multiple adult $CD4^+$ T-cell subsets at single-cell resolution (Fig. 6D). Within this pathway, our analyses highlighted a seven-TF module - FOS, FOSL1, FOSL2, MAFF, EGR1, EGR2 and NR4A3 – that forms a core node of TNFα/NF-κB network significantly downregulated in T1D Treg cells (Fig. 1D; **Table S1**), with AP-1 family members FOS/FOSL1/FOSL2 also showing decreased TF footprints in DA enhancers, consistent with their down-regulation at the mRNA level (Fig. 3A, B). We therefore asked whether combinatorial knockdown of this TF module in healthy human Treg would shift their transcriptional state toward the T1D programmes defined above. Using the multiplexed effector guide arrays (MEGA) CRISPR-RfxCas13d system [45] we multiplexed knockdown (KD) of all seven TFs in healthy adult primary Treg cells (**Supplementary Fig. 4A**), and compared these cells to control cells expressing RfxCas13d and a non-targeting (NT) control guide (Fig. 7). Semi quantitative PCR confirmed significant reductions in transcript abundance for *FOS*, *FOSL1*, *FOSL2*, *EGR1*, *EGR2* with *MAFF* and *NR4A3* showing non-significant modest changes in the KD group (Fig. 7A). Bulk RNA-seq confirmed concordant decreases in $\log_2$ counts-per-million for the majority of targeted TFs (6/7 except for FOSL1) in KD cells relative to NT controls (Fig. 7B), indicating that the muti gene targeting effectively suppresses the module at multiple points. Expression of key Treg identity markers including *FOXP3*, *CD25* and *CTLA*-4 remained stable (**Supplementary Fig. 4B**), suggesting that the perturbation affects regulatory circuitry without destabilising the Treg lineage, in line with Treg RNA-seq data from our paediatric T1D cohort. Differential expression analysis between KD and NT identified 237 DE genes (131 down, 106 up; FDR < 0.05) (Fig. 7C) and GSEA revealed 10 significantly enriched gene sets (FDR < 0.1), including downregulation of TNFα signalling via NF-κB, estrogen response early, IL6–JAK–STAT3 signalling, hedgehog signalling and interferon/inflammatory response (Fig. 7D). To evaluate how closely these changes resemble the T1D signatures, we compared the GSEA KD results with paediatric Treg RNA-seq. Five out of the six gene sets downregulated in healthy Treg KD, including TNFα signalling via NF-κB, inflammatory response, IL6–JAK–STAT3 signalling, hedgehog signalling and estrogen response early, were also significantly downregulated in the paediatric T1D dataset (**Fig. 9E,F**). These shared pathways were strongly correlated between healthy Treg KD and T1D Treg data (Spearman $\rho \approx 0.9$; **Fig. 9E**), and the leading-edge/top-contributing genes within each pathway showed significant overlap between two datasets, with Jaccard indices significantly greater than expected by chance (Fisher's exact test, ****$P < 5 \times 10^{-6}$; **Fig. 9H**). A heatmap of all pathways significantly enriched in either dataset further reinforced that most pathways altered by KD in healthy Treg move in the same direction as in paediatric T1D Treg cells (**Fig. 9G**). Together, these show that subtle, coherent reductions in the TNFα/NF-κB network created from multiplex KD of a seven-TF module is sufficient to drive healthy Treg toward a transcriptional state that mirrors the pathway-level changes

seen in T1D Treg. This reinforces the power of integrating chromatin, 3D genome, bulk and single-cell transcriptomic data with targeted RNA-level perturbation to move from association to mechanism.

Discussion

Type 1 diabetes (T1D) is a condition of subtle, distributed immune dysregulation rather than a single breakdown point. Genetic studies show that most T1D risk variants lie in non-coding enhancers active in $CD4^+$ T cells [8–11], suggesting perturbed regulation in these cells rather than obvious defects in core lineage genes such as FOXP3, which is not a T1D susceptibility gene [46, 47]. In order to identify the key gene changes that may be therapeutic targets to delay or prevent T1D, we set out to map those regulatory networks in paediatric T cells subsets, and determine whether we could move beyond correlations to a more mechanistic understanding of how enhancer changes tune T-cell programmes in T1D.

We address several limitations of previous omics studies in T1D. Most prior work has focused on bulk $CD4^+$ T-cell or unfractionated PBMC profiles [15–17] with fewer Treg-focussed studies, due to the scarcity of Treg in blood (> 5% of PBMC). Current T1D epigenomic and transcriptomic studies profile resting T cells [18–25], which will not capture stimulation-dependent regulatory effects, and this is critical as many T-cell risk loci and enhancers containing T1D variants are either amplified by or only detectable after T cell activation [11, 26, 27, 48]. Furthermore, matched chromatin accessibility and gene expression measurements in this context have not been reported, especially from children using cryopreserved T1D biobank material. This kind of design is particularly challenging due to limited input of biobank resources and the rarity of subsets such as Treg cells. By adapting our parallel ATAC/RNA workflow optimised for low-input Treg we previously described [49], we can directly relate accessibility changes in paediatric Treg and Tconv cells to their transcriptomic changes.

The first observation is that T1D is associated with widespread chromatin and transcriptional changes in $CD4^+$ Tconv and Treg lineages. Classic core Treg markers remain enriched in T1D Treg, confirming a published transcriptomic study reporting that their signature in T1D is only subtly perturbed [23]. Instead, we see numerous small changes in accessibility and gene expression across both Treg and Tconv cells, with subtle Treg/Tconv distinctions and shared pathways across subsets. This supports a polygenic and omnigenic model, where cumulative modest perturbations distributed across gene networks, rather than a single dominant defect, shapes autoimmune risk [50, 51]. This suggests that in T1D, and likely other autoimmune diseases, tolerance is not broken by a single switch, but by a coordinated de-tuning of multiple regulatory controls. This is consistent with other studies [18, 22] including Niederlova, Neuwirth [24] who reported that differential expression patterns in T1D across T-cell subsets are subtle and largely concordant, with only a small number of select genes showing distinct subset-specific regulation. Similarly, parallel profiling of Treg and Tconv transcriptomes in T1D from Ferraro, D'Alise [23] demonstrated that the overall Treg signature is only subtly perturbed in T1D, suggesting that differences may simply reflect a different tuning in expression.

A second finding is the convergence of multiple layers of evidence for disruption of a specific regulatory axis involving TNFα/NF-κB, AP-1 factors and MAF. Across ATAC-seq, TF footprinting and RNA-seq, we repeatedly see attenuation of TNFα/NF-κB-linked and AP-1-driven programmes in T1D Treg/Tconv cells. TF motifs for FOS/FOSL1/FOSL2::JUNB show reduced local accessibility, and transcripts such as *FOSL2*, *MAFF*, *EGR1*, *EGR2* and *NR4A3* are themselves diminished in T1D Treg. Consistent with our findings, downregulated expression of FOS members has been reported in multiple T1D T-cell subsets compared to healthy [24]. These same factors have well-described roles in normal Treg development [52], Th17 restraint and negative selection [38, 53], IL-10 production [54, 55], making them plausible routes through which modest non-coding changes could translate into broader tolerance defects.

At first sight this seems at odds with the traditional view of T1D as a condition of heightened TNFα/NF-κB and interferon signalling [18, 20, 56]. However, recent single-cell profiling of new-onset T1D and LADA refines this view [20], describing a mixed inflammatory-inhibitory state that suggests heightened activation or chronic antigenic stimulation. In our datasets, we observed reduced accessibility at AP-1 family motifs and expression of immediate-early response genes typically induced by cell activation. Because AP-1 and TNF are normally rapidly induced upon activation, including by CD3/CD28 agonism [57–59], the reduced signals we observe in our data likely reflect a pre-existing sustained and amplified chronic antigenic/cytokine exposure leading to an exhaustion state. This suggests the cells are not grossly dysfunctional but are “tuned down”, such that they may still respond but at a reduced capacity. Such tuning may reflect negative feedback from chronic autoantigen exposure or intrinsic deficits in activation pathways that is accumulated as a result of longitudinal exposure to environmental cues.

Analysis of an independent adult single-cell PBMC dataset reinforced the dysregulation of the same TNF/MAF/MAFF gene signature observed in our primary analysis of the paediatric T1D cohort. Despite differences in cohort, age and technology, we again saw downregulation of a TNF/MAF/MAFF gene module and common pathways across multiple T cell subsets. Notably, the direction of T1D vs control $\log_2$ fold-change in adult transitional cluster was concordant with that in our adolescent bulk Tconv RNA-seq, with these same genes (*MAFF*, *RORC*, *TNF*, *BNIPL*, *PRSS23*, *ZNF90*) significantly downregulated in our paediatric bulk Tconv RNA-seq. *TNF* transcripts were also downregulated in a broad range of subpopulations including adult T1D memory, naïve CD4⁺ T-cell and proliferating T cells (Fig. 1C-D, 6C, Supplementary Fig. 3). These data indicate that despite differences in age and sampling context, a common programme is dysregulated in T1D, affecting both the frequency of a transitional CD4⁺ state and the expression level of its defining genes. These cross-cohort, cross-modality consistencies argue that the signature we describe reflects a shared T1D-linked network in circulating CD4⁺ T cells. This also reinforces recent single-cell work in paediatric and adult cohorts showing that T1D is associated with selective modulation of specific CD4⁺ states [15, 19, 24, 25], such as cytotoxic [15] or transitional antigen-specific subset [25], rather than uniform shifts across all CD4⁺ T cells.

A third advance is our use of T cell Hi-C maps to connect non-coding changes to their contact genes in 3D space. GWAS and enhancer mapping have convincingly shown that T1D risk variants are enriched in distal enhancers active in CD4⁺ T cells [8, 11, 22], but linking these elements to their long-range targets

has been challenging. We show here that incorporating 3D contacts from adult Treg and CD4⁺ Hi-C as a scaffold improved concordance between altered enhancer accessibility and target gene expression. Several altered enhancers loop to the promoters of *TNF*, *IL2*, *IL10RB*, *IL17F*, *ICAM1* and *MAF*, targets that would have been annotated differently using proximity-based assignment. Notably, although 3D mapping reshuffles individual gene assignments, TNF signalling still emerges as one of the strongest connected nodes, reinforcing a dominant TNFα/NF-κB–centred network underlying the enhancer changes. Although our Hi-C is derived from healthy adult donors, these analyses provide a proof of principle that T1D-altered enhancers can be meaningfully connected to disease-relevant genes using 3D maps, improving our interpretation beyond what linear proximity allows.

Our findings are consistent with prior work reporting altered TNF-α [19, 20, 60–62] and interferon signalling [17, 19, 63] in peripheral immune cells from individuals with T1D. Recent single-cell work by Golodnikov, Podshivalova [20] also highlighted a pan-lineage alteration of TNF/NF-κB and JAK-STAT signaling in newly diagnosed T1D and indolent latent autoimmune diabetes in adults (LADA) that aligns with our findings in our T1D cohort. Although, correlation across multiple omics implicates the TNFα/NF-κB network in Treg this does not by itself establish causality. This requires highly targeted functional genomics approaches now possible in primary human T cells. The repeated appearance of the TNFα/NF-κB modules across chromatin and expression layers, in both Tconv and Treg cells, prompted subsequent analyses and CRISPR–Cas13d functional perturbation experiments.

Central to the T1D regulatory architecture uncovered in this study is a seven-TF module - FOS, FOSL1, FOSL2, MAFF, EGR1, EGR2 and NR4A3, that forms a core node of the TNFα/NF-κB network in Treg. These factors have been individually implicated in Treg differentiation, stability or tolerance induction [52, 54, 55, 64], but in T1D they are subtly and collectively reduced, rather than absent. By using MEGA CRISPR–Cas13d [45] to multiplex knockdown of all seven TFs in primary human Treg, we tested whether downregulation of the TNFα/NF-κB–linked TF we identified are sufficient to “stress” healthy Treg toward a T1D-like transcriptional state. Cas13d targeting of mRNA without editing DNA, provided a closer approximation to the partial reductions observed in our transcriptomics data rather than the severely reduce to complete absence caused by editing the genes themselves. Rather strikingly, even with moderate knockdown, we saw a pathway-level phenotype that closely mirrors the T1D patient data including reduced TNFα/NF-κB, inflammatory response, IL6–JAK–STAT3 and hedgehog signalling, and a significant overlap in the leading-edge genes driving these enrichments. At the same time, Treg key lineage markers remained stable, again reinforcing that T1D perturbations tune regulation rather than destabilising Treg identity [23]. Given that these pathway level changes are acquired over many years of cumulative risk exposure in T1D, that fact that they are recapitulated in healthy human Treg over days, suggests the power of these changes to drive loss of tolerance. This supports an omnigenic model in which multiple modest regulatory perturbations collectively reshape immune pathways and converge on shared regulatory circuits. Our data support a model of pathway-level tuning in which cumulative small changes alter transcriptional set-points in CD4⁺ T cells.

These findings have implications for refining the role of TNF biology and therapy in T1D. TNF has a dual role in autoimmunity: early in disease it can accelerate β-cell death, whereas later it can promote deletion of autoreactive T cells and stabilisation of Treg via TNFR2 [56, 60, 65–68]. Clinical trials with anti-TNF agents such as etanercept and golimumab show benefits in preserving C-peptide in new-onset T1D, whereas approaches that increase TNF or enhance TNFR2 signalling (e.g. BCG vaccination or TNFR2 agonists) may benefit individuals with long-standing disease [69–71]. We observed a blunted TNFα/NF-κB/AP-1 response in stimulated $CD4^+$ T cells and downregulating this in healthy cells confirms a T1D-like transcriptional state. This suggests that TNF therapies may have very different consequences depending on the cell state and the balance of effector and Treg cells, and carefully timed restoration rather than inhibition could be beneficial.

Methodologically, we show how multi-layer data can move from association to mechanism in a complex human disease, by integrating parallel ATAC/RNA-seq from cryopreserved, rare paediatric T cells with TF footprint, Hi-C-based enhancer-gene linking, independent single-cell RNA-seq and multiplex CRISPR–Cas13d perturbation to reconstruct altered regulatory networks in T1D $CD4^+$ T cells. This approach is broadly applicable to other autoimmune diseases in which non-coding risk in immune cells is prominent.

In terms of limitations, our Hi-C integration relies on healthy adult T cells rather than paediatric samples, as 3D genome maps in primary T-cell subsets are currently available exclusively from adults. The development of sensitive low input Hi-C and related assays may address this in the future. Our analysis is therefore a proof-of-concept use of 3D architecture as a scaffold to interpret enhancer changes and highlight a subset of targets where chromatin, 3D structure and transcription all point to the same dysregulation. A further limitation is that the samples used for multi-omic profiling were not genotyped so we could not directly link individual T1D risk variants to the observed changes. Furthermore, the CRISPR perturbation experiments were performed in adult Treg and we did not directly measure suppressive function or *in vivo* efficacy. Despite these caveats, the convergence we observe across multiple omics strongly supports a model in which a TNFα/NF-κB/AP-1-centred module is attenuated across in T1D $CD4^+$ T cells. Our work reinforces mis-tuned regulatory circuitry in T1D as the driver of disease progression and provides a framework for testing cell-type-targeted interventions aimed at restoring regulatory balance in T1D. For prevention, these may be most effective when delivered early to at risk children based on population screening and GRS, and for treatment, delivery before overt destruction of the beta cells has progressed.

Methods

Paediatric cohort and ethics. Children were recruited as part of the Australian Type 1 Diabetes and the Gut (TIGs) cohort, a prospective study of youth with islet autoimmunity (IA) or recent-onset type 1 diabetes (T1D) and autoantibody-negative controls [33, 34]. For this study, we selected 12 children with T1D and 12 autoantibody-negative controls. Blood was collected at the Women's and Children's Hospital, Adelaide, Australia (Ethics approval 1596/08/2019). PBMCs were isolated by Ficoll density gradient,

cryopreserved in 90% FCS/10% DMSO and stored in liquid nitrogen. Written informed consent was obtained according to local guidelines.

PBMC thawing, T-cell sorting and stimulation. Cryovials were rapidly thawed at 37°C, diluted dropwise into pre-warmed X-VIVO 15 medium supplemented with 2 mM HEPES, 2 mM L-glutamine, 5% heat-inactivated human serum and 200 U/mL DNase I, then washed twice in media and rested overnight in the same media without DNase I at ~ 3.5–4.0 × 10^6 cells/mL at 37°C, 5% CO_2. Viability was assessed by trypan blue following the overnight rest with only samples with ≥ 90% viability used. The following day, PBMCs were stained with a viability stain (Fixable Viability Stain 700) plus anti-CD4, anti-CD25 and anti-CD127. Viable Treg were sorted as $CD4^+CD25^{hi}CD127^{lo}$, and Tconv as $CD4^+CD25^{lo}CD127^{hi}$ on a BD FACSAria Fusion. Post-sort purity was routinely > 95%. Cells were cultured in complete X-VIVO 15 with 500 U/mL recombinant human IL-2 and stimulated for 48h with anti-CD3/CD28 Dynabeads (1:1 bead:cell ratio). Beads were removed by magnetic separation before ATAC-seq and RNA-seq preparation.

Parallel Omni-ATAC and RNA-seq. Chromatin accessibility profiling was performed using an Omni-ATAC protocol adapted for cryopreserved primary human T cells and parallel gene expression profiling as described in Wong, Harbison [49]. In brief, 1.1–5 × 10^4 stimulated Treg or Tconv were pre-treated with DNase I, lysed in ice-cold resuspension buffer containing NP-40, Tween-20 and digitonin, and nuclei were pelleted. The supernatant containing cytoplasmic RNA was collected, mixed with TRIzol LS and frozen at − 80°C for matched RNA-seq. Nuclei were tagmented in 2× TD buffer with Tn5 transposase at 37°C for 30 min, and DNA was purified, size-selected (100–800 bp) and amplified to generate indexed libraries. Libraries were quantified and sequenced (Illumina HiSeq, 2 × 150 bp) to a mean depth of ~ 30 million paired reads per sample. Total RNA was extracted from ATAC supernatants using the miRNeasy Micro kit (Qiagen). Samples were subjected to poly(A) selection and library construction with the NEBNext Ultra II Directional RNA Library Prep Kit (NEB), followed by 2 × 150 bp sequencing on Illumina HiSeq to a mean depth of ~ 26 million paired reads per sample.

ATAC-seq processing, differential accessibility and TF footprinting. ATAC reads were adapter-trimmed with cutadapt and aligned to GRCh37 using Bowtie2 with a maximum fragment length of 2 kb. PCR duplicates, mitochondrial reads and reads in ENCODE blacklisted regions were removed. Tn5 insertion sites were offset ± 4/5 bp to centre transposase binding. Peaks were called on pooled Treg or Tconv BAM files using MACS2 (BAMPE mode, fixed 500-bp peaks around summits). Sex-chromosome peaks were excluded to avoid confounding from sex-specific copy number. A consensus peak set was built across samples, and read counts per peak were obtained with csaw. Low-count peaks were filtered. For differential accessibility, testing was restricted to enhancer-annotated peaks [9] to focus on distal regulatory elements, and T1D–control differences were assessed using edgeR with TMM normalisation and dispersion estimation. RUVSeq was used to estimate and regress unwanted variation based on empirical control regions. Peaks with FDR < 0.05 were considered differentially accessible (DA). TF footprints were inferred with HINT-ATAC [72], using pooled (by T1D/healthy) reads from nucleosome-free (< 146 bp) and mononucleosomal (146–307 bp) fragments, and matched to JASPAR motif PWMs. HINT-

ATAC differential mode was used to identify motifs with significant differences in TF activity between T1D and controls.

RNA-seq processing and differential expression. RNA-seq reads were adapter-trimmed and aligned to GRCh38 using STAR [73], retaining uniquely mapped reads. Gene-level counts were generated with featureCounts [74] using GENCODE annotations. Genes with low expression (≤ 1 count per million in most samples) were removed. Differential expression (DE) was assessed with edgeR/limma-voom [75]. Normalisation factors were estimated by TMM, voom was used to model mean–variance relationships, and RUVSeq-derived factors [76] were included to control unwanted variation alongside donor pairing and disease status. Genes with Benjamini–Hochberg FDR < 0.05 were called DE.

Hi-C–guided enhancer–gene mapping. To link DA peaks to distal targets, we intersected DA regions with significant Hi-C interactions (minCount ≥ 5 or CHiCAGO score ≥ 5) identified from published Hi-C map of human primary Treg [13] and pcHi-C map of activated human $CD4^+$ T cells [12]. DA peaks overlapping Hi-C interactions were assigned to genes whose promoters they contacted. We designated a "3D reassignment" where the Hi-C-linked gene differed from the nearest TSS in linear distance, and then overlapped these genes with DE genes from our Treg and Tconv RNA-seq to identify candidate 3D-connected effector genes.

Adult single-cell RNA-seq analysis. We analysed raw scRNA-seq data generated by Parse Biosciences from 22 adult PBMC samples (12 T1D, 10 controls) processed in a single Evercode Whole Transcriptome Mega run (> 1 million barcoded cells). FASTQ files were processed with the Parse v0.9.6 pipeline to produce cell-by-gene count matrices. Downstream analysis used standard single-cell workflows from Seurat [77]. Low-quality cells (high mitochondrial fraction, low gene counts) and doublet-enriched barcodes were removed. Data were normalised, log-transformed and integrated across donors. Clusters were identified by graph-based clustering and annotated using canonical markers into major PBMC populations, and then subclustered into $CD4^+$ T-cell subsets (naïve, memory, transitional, Treg, proliferating).

MEGA CRISPR–Cas13d perturbation. The MEGA CRISPR-RfxCas13d system described in Tieu, Sotillo [45] was used for multiplexed transcriptome editing of seven TFs in primary human Treg cells. Treg cells were isolated from adult buffy coats obtained from the Australian Red Cross (Ethics approval #33087) by CD4 enrichment followed by FACS of $CD4^+CD25^{hi}CD127^{lo}$ cells. Cells were cultured in X-VIVO 15 with IL-2/IL-7 and activated with CD3/CD28 Dynabeads. Cells were co-transduced with a constitutively active Cas13d lentiviral vector and a multiplex guide array targeting *FOS*, *FOSL1*, *FOSL2*, *MAFF*, *EGR1*, *EGR2* and *NR4A3*, or a non-targeting (NT) control array, at a combined MOI of 25. After expansion and puromycin selection, $mCherry^+$ transduced Treg were purified by FACS. Knockdown efficiency for each TF was quantified by RT-qPCR and RNA-seq libraries (4 KD and 4 NT samples) were prepared with NEBNext Ultra II Directional kits as above and sequenced to ~ 40 million paired reads per sample. DE analysis between knockdown and control Treg followed the same pipeline as for paediatric RNA-seq.

Pathway and statistical analysis. Pathway analysis for bulk RNA-seq, ATAC-seq single-cell subsets and CRISPR perturbation was performed using GSEA on ranked gene lists (log_2 fold-change), focusing on Hallmark gene sets. Normalised enrichment scores and FDR-adjusted q values were reported. Additional statistics (e.g. Fisher's exact tests, Spearman correlations) were performed in R; two-sided tests with $P < 0.05$ or FDR < 0.05 were considered significant unless otherwise stated.

Declarations

Acknowledgements

We thank Benjamin Ramoso, Alison Gwiazdzinski and Sarah Beresford (ENDIA Study, WCH) for their assistance in blood collection. We would like to thank all the volunteers who consented to giving blood for this study. We thank Dr. Randall Grose (SAHMRI Research and Core Facilities) for cell isolation and flow cytometry expertise, Dr. Stephen Wilcox (WEHI Genomics Hub) and Genewiz for Illumina sequencing. We acknowledge the South Australian Genomics Centre (SAGC) which provided sequencing service. The SAGC is supported by the National Collaborative Research Infrastructure Strategy (NCRIS) via Bioplatforms Australia and by the SAGC partner institutes. We thank Parse Biosciences for providing access to the adult T1D single-cell RNA-seq dataset, and Dr. Charlie Roco and Nicole Carter for their support and discussions. Part of this work was supported by the Environmental Determinants of Islet Autoimmunity (ENDIA) Study. The ENDIA Study was supported by Breakthrough T1D Australia, the recipient of the Commonwealth of Australia grant for Accelerated Research under the Medical Research Future Fund, and with funding from The Leona M. and Harry B. Helmsley Charitable Trust (grant # 3-SRA-2020-966-M-N). In addition, part of this grant was also funded by a Women's and Children's Hospital Research Foundation grant (Sadlon and Barry).

Author contributions

Y.Y.W. contributed to the acquisition, analysis and integration of ATAC-seq, RNA-seq and scRNA-seq datasets and manuscript writing. C.M.H. contributed to the design of flow cytometry and immune cell sorting. J.E.H. and J.J.C. contributed to PBMC collection and biobanking methodology. B.G. contributed to cell culture methodology. J.A.G. contributed to the generation of lentiviral constructs used in the MEGA CRISPR–Cas13d system. D.H. optimised and performed the MEGA CRISPR–Cas13d perturbation experiments. M.B., J.S., M.K., K.H. and S.P. provided ATAC-seq training and guidance on ATAC-seq sequencing and data analysis. Y.Y.W. performed the data analyses for this study with input from J.B., N.L., S.M.P. and S.W.W. T.S. and S.C.B. supervised the experiments and contributed to data interpretation and critical revision of the manuscript. S.C.B. directed the project, obtained funding and provided overall supervision and resources.

Availability of data and materials

The datasets supporting the conclusions of this article are available in the European Nucleotide Archive (ENA) repository, [PRJ X in https:// Y].

References

1. Burrack AL, Martinov T, Fife BT. T Cell-Mediated Beta Cell Destruction: Autoimmunity and Alloimmunity in the Context of Type 1 Diabetes. Front Endocrinol (Lausanne). 2017;8:343.
2. Fousteri G, et al. Following the fate of one insulin-reactive CD4 T cell: conversion into Teffs and Tregs in the periphery controls diabetes in NOD mice. Diabetes. 2012;61(5):1169–79.
3. Golden GJ, et al. Immune perturbations in human pancreas lymphatic tissues prior to and after type 1 diabetes onset. Nat Commun. 2025;16(1):4621.
4. Viisanen T, et al. FOXP3 + Regulatory T Cell Compartment Is Altered in Children With Newly Diagnosed Type 1 Diabetes but Not in Autoantibody-Positive at-Risk Children. Front Immunol. 2019;10:19.
5. Lindley S, et al. Defective suppressor function in CD4(+)CD25(+) T-cells from patients with type 1 diabetes. Diabetes. 2005;54(1):92–9.
6. Schneider A, et al. The effector T cells of diabetic subjects are resistant to regulation via CD4 + FOXP3+ regulatory T cells. J Immunol. 2008;181(10):7350–5.
7. Onengut-Gumuscu S et al. Type 1 Diabetes Genetics Consortium. J Clin Endocrinol Metabolism, 2025: p. dgaf181.
8. Onengut-Gumuscu S, et al. Fine mapping of type 1 diabetes susceptibility loci and evidence for colocalization of causal variants with lymphoid gene enhancers. Nat Genet. 2015;47(4):381–6.
9. Vahedi G, et al. Super-enhancers delineate disease-associated regulatory nodes in T cells. Nature. 2015;520(7548):558–62.
10. Farh KK-H, et al. Genetic and epigenetic fine mapping of causal autoimmune disease variants. Nature. 2015;518(7539):337–43.
11. Robertson CC, et al. Fine-mapping, trans-ancestral and genomic analyses identify causal variants, cells, genes and drug targets for type 1 diabetes. Nat Genet. 2021;53(7):962–71.
12. Javierre BM, et al. Lineage-Specific Genome Architecture Links Enhancers and Non-coding Disease Variants to Target Gene Promoters. Cell. 2016;167(5):1369–e138419.
13. Liu N, et al. 3DFAACTS-SNP: using regulatory T cell-specific epigenomics data to uncover candidate mechanisms of type 1 diabetes (T1D) risk. Volume 15. Epigenetics & Chromatin; 2022. p. 24. 1.
14. Mumbach MR, et al. Enhancer connectome in primary human cells identifies target genes of disease-associated DNA elements. Nat Genet. 2017;49(11):1602–12.
15. Bediaga NG, et al. Cytotoxicity-Related Gene Expression and Chromatin Accessibility Define a Subset of CD4 + T Cells That Mark Progression to Type 1 Diabetes. Diabetes. 2022;71(3):566–77.
16. Kallionpää H, et al. Early Detection of Peripheral Blood Cell Signature in Children Developing β-Cell Autoimmunity at a Young Age. Diabetes. 2019;68(10):2024–34.
17. Suomi T et al. Gene expression signature predicts rate of type 1 diabetes progression. eBioMedicine, 2023. 92.

18. Abedi M, et al. Joint profiling of gene expression and chromatin accessibility in pancreatic lymph nodes and spleens in human type 1 diabetes. Sci Immunol. 2025;10(113):eadz0472.
19. Honardoost MA, et al. Systematic immune cell dysregulation and molecular subtypes revealed by single-cell RNA-seq of subjects with type 1 diabetes. Genome Med. 2024;16(1):45.
20. Golodnikov II et al. Single-cell immune transcriptomics reveals an inflammatory-inhibitory set-point spectrum in autoimmune diabetes. JCI Insight, 2026. 11(1).
21. Biradar R, et al. Single-cell RNA-seq analysis of longitudinal CD4(+) T cell samples reveals cell-type-specific changes during early stages of type 1 diabetes. Genome Med. 2025;17(1):154.
22. Gao, P., et al., *Risk variants disrupting enhancers of T_H1 and T_{REG}cells in type 1 diabetes.* Proceedings of the National Academy of Sciences, 2019. 116(15): p. 7581.
23. Ferraro A et al. *Interindividual variation in human T regulatory cells.* Proceedings of the National Academy of Sciences, 2014. 111(12): pp. E1111-E1120.
24. Niederlova V, et al. Imbalance of stem-like and effector T cell states in children with early type 1 diabetes across conventional and regulatory subsets. Nat Commun. 2025;16(1):11301.
25. Eugster A, et al. Physiological and pathogenic T cell autoreactivity converge in type 1 diabetes. Nat Commun. 2024;15(1):9204.
26. Schmiedel BJ, et al. Single-cell eQTL analysis of activated T cell subsets reveals activation and cell type-dependent effects of disease-risk variants. Sci Immunol. 2022;7(68):eabm2508.
27. Soskic B, et al. Immune disease risk variants regulate gene expression dynamics during CD4 + T cell activation. Nat Genet. 2022;54(6):817–26.
28. Holcar M et al. *Age-Related Differences in Percentages of Regulatory and Effector T Lymphocytes and Their Subsets in Healthy Individuals and Characteristic STAT1/STAT5 Signalling Response in Helper T Lymphocytes.* J Immunol Res, 2015. 2015: p. 352934.
29. Gheitasi R, et al. Age- and sex-associated differences in immune cell populations. iScience. 2025;28(8):113092.
30. Dietz S, et al. Expression of immune checkpoint molecules on adult and neonatal T-cells. Immunol Res. 2023;71(2):185–96.
31. Connors, T.J., et al., *Site-specific development and progressive maturation of human tissue-resident memory T cells over infancy and childhood.* Immunity, 2023. 56(8): pp. 1894–1909.e5.
32. Petrov L, et al. Rewired type I IFN signaling is linked to age-dependent differences in COVID-19. Cell Rep Med. 2025;6(8):102285.
33. Harbison JE, et al. Gut microbiome dysbiosis and increased intestinal permeability in children with islet autoimmunity and type 1 diabetes: A prospective cohort study. Pediatr Diabetes. 2019;20(5):574–83.
34. Harbison JE, et al. Associations between diet, the gut microbiome and short chain fatty acids in youth with islet autoimmunity and type 1 diabetes. Pediatr Diabetes. 2021;22(3):425–33.

35. Long SA, et al. Defects in IL-2R Signaling Contribute to Diminished Maintenance of FOXP3 Expression in CD4 + CD25+ Regulatory T-Cells of Type 1 Diabetic Subjects. Diabetes. 2009;59(2):407–15.
36. Sadlon TJ, et al. Genome-wide identification of human FOXP3 target genes in natural regulatory T cells. J Immunol. 2010;185(2):1071–81.
37. Uno S, et al. Expression of chemokines, CXC chemokine ligand 10 (CXCL10) and CXCR3 in the inflamed islets of patients with recent-onset autoimmune type 1 diabetes. Endocr J. 2010;57(11):991–6.
38. Imbratta C, et al. Maf deficiency in T cells dysregulates Treg - TH17 balance leading to spontaneous colitis. Sci Rep. 2019;9(1):6135.
39. Alam MS et al. *TNF plays a crucial role in inflammation by signaling via T cell TNFR2.* Proc Natl Acad Sci U S A, 2021. 118(50).
40. Shen L, et al. The apoptosis-associated protein BNIPL interacts with two cell proliferation-related proteins, MIF and GFER. FEBS Lett. 2003;540(1–3):86–90.
41. Dolton G et al. HLA A*24:02-restricted T cell receptors cross-recognize bacterial and preproinsulin peptides in type 1 diabetes. J Clin Invest, 2024. 134(18).
42. Koufakis T, et al. Interleukin-6-Related Inflammatory Burden in Type 1 Diabetes: Evidence for Elevation with Suboptimal Glycemic Control. J Clin Med. 2025;14:6511. 10.3390/jcm14186511.
43. Mittal R et al. Interplay of hypoxia, immune dysregulation, and metabolic stress in pathophysiology of type 1 diabetes. Front Immunol, 2025. Volume 16–2025.
44. Fagundes RR, Zaldumbide A, Taylor CT. Role of hypoxia-inducible factor 1 in type 1 diabetes. Trends Pharmacol Sci. 2024;45(9):798–810.
45. Tieu, V., et al., *A versatile CRISPR-Cas13d platform for multiplexed transcriptomic regulation and metabolic engineering in primary human T cells.* Cell, 2024. 187(5): pp. 1278–1295.e20.
46. Bjørnvold M, et al. FOXP3 polymorphisms in type 1 diabetes and coeliac disease. J Autoimmun. 2006;27(2):140–4.
47. Zavattari P, et al. No Association Between Variation of the FOXP3 Gene and Common Type 1 Diabetes in the Sardinian Population. Diabetes. 2004;53(7):1911–4.
48. Calderon D, et al. Landscape of stimulation-responsive chromatin across diverse human immune cells. Nat Genet. 2019;51(10):1494–505.
49. Wong YY, et al. Parallel recovery of chromatin accessibility and gene expression dynamics from frozen human regulatory T cells. Sci Rep. 2023;13(1):5506.
50. Boyle EA, Li YI, Pritchard JK. An Expanded View of Complex Traits: From Polygenic to Omnigenic. Cell. 2017;169(7):1177–86.
51. Iakovliev A, et al. Genome-wide aggregated trans-effects on risk of type 1 diabetes: A test of the omnigenic sparse effector hypothesis of complex trait genetics. Am J Hum Genet. 2023;110(6):913–26.

52. Koizumi SI, et al. JunB regulates homeostasis and suppressive functions of effector regulatory T cells. Nat Commun. 2018;9(1):5344.
53. Shetty A, et al. A systematic comparison of FOSL1, FOSL2 and BATF-mediated transcriptional regulation during early human Th17 differentiation. Nucleic Acids Res. 2022;50(9):4938–58.
54. Cox LS, et al. Blimp-1 and c-Maf regulate Il10 and negatively regulate common and unique proinflammatory gene networks in IL-12 plus IL-27-driven T helper-1 cells. Wellcome Open Res. 2023;8:403.
55. Xu J, et al. c-Maf regulates IL-10 expression during Th17 polarization. J Immunol. 2009;182(10):6226–36.
56. Dos Santos Haber JF et al. The Relationship between Type 1 Diabetes Mellitus, TNF-α, and IL-10 Gene Expression. Biomedicines, 2023. 11(4).
57. Chauhan D, et al. Regulation of c-jun Gene Expression in Human T Lymphocytes. Blood. 1993;81(6):1540–8.
58. Ferran C, et al. Cytokine-related syndrome following injection of anti-CD3 monoclonal antibody: further evidence for transient in vivo T cell activation. Eur J Immunol. 1990;20(3):509–15.
59. Scott DE, et al. Anti-CD3 antibody induces rapid expression of cytokine genes in vivo. J Immunol. 1990;145(7):2183–8.
60. Ban L, et al. Selective death of autoreactive T cells in human diabetes by TNF or TNF receptor 2 agonism. Proc Natl Acad Sci U S A. 2008;105(36):13644–9.
61. Foss NT, et al. Impaired cytokine production by peripheral blood mononuclear cells in type 1 diabetic patients. Diabetes Metab. 2007;33(6):439–43.
62. Vitali L, et al. Low serum TNF-alpha levels in subjects at risk for type 1 diabetes. J Pediatr Endocrinol Metab. 2000;13(5):475–81.
63. Ferreira RC, et al. A type I interferon transcriptional signature precedes autoimmunity in children genetically at risk for type 1 diabetes. Diabetes. 2014;63(7):2538–50.
64. Morita K, et al. Egr2 and Egr3 in regulatory T cells cooperatively control systemic autoimmunity through Ltbp3-mediated TGF-β3 production. Proc Natl Acad Sci U S A. 2016;113(50):E8131–40.
65. Faustman D, Davis M. TNF receptor 2 pathway: drug target for autoimmune diseases. Nat Rev Drug Discov. 2010;9(6):482–93.
66. Chen X, et al. TNFR2 is critical for the stabilization of the CD4 + Foxp3+ regulatory T. cell phenotype in the inflammatory environment. J Immunol. 2013;190(3):1076–84.
67. Faustman DL. TNF, TNF inducers, and TNFR2 agonists: A new path to type 1 diabetes treatment. Diabetes Metab Res Rev, 2018. 34(1).
68. Christen U, et al. A dual role for TNF-alpha in type 1 diabetes: islet-specific expression abrogates the ongoing autoimmune process when induced late but not early during pathogenesis. J Immunol. 2001;166(12):7023–32.

69. Rigby MR, et al. Two-Year Follow-up From the T1GER Study: Continued Off-Therapy Metabolic Improvements in Children and Young Adults With New-Onset T1D Treated With Golimumab and Characterization of Responders. Diabetes Care. 2023;46(3):561–9.
70. Faustman DL, et al. Proof-of-concept, randomized, controlled clinical trial of Bacillus-Calmette-Guerin for treatment of long-term type 1 diabetes. PLoS ONE. 2012;7(8):e41756.
71. Mastrandrea L, et al. Etanercept Treatment in Children With New-Onset Type 1 Diabetes: Pilot randomized, placebo-controlled, double-blind study. Diabetes Care. 2009;32(7):1244–9.
72. Li Z, et al. Identification of transcription factor binding sites using ATAC-seq. Genome Biology. 2019;20(1):45.
73. Dobin A, et al. STAR: ultrafast universal RNA-seq aligner. Bioinformatics. 2013;29(1):15–21.
74. Liao Y, Smyth GK, Shi W. featureCounts: an efficient general purpose program for assigning sequence reads to genomic features. Bioinformatics. 2014;30(7):923–30.
75. Robinson MD, McCarthy DJ, Smyth GK. edgeR: a Bioconductor package for differential expression analysis of digital gene expression data. Bioinformatics. 2010;26(1):139–40.
76. Risso D, et al. Normalization of RNA-seq data using factor analysis of control genes or samples. Nat Biotechnol. 2014;32(9):896–902.
77. Butler A, et al. Integrating single-cell transcriptomic data across different conditions, technologies, and species. Nat Biotechnol. 2018;36(5):411–20.

Tables

Table 1 | **Demographic and sample characteristics of the paediatric multi-omics cohort.**
Data are shown for children with Type 1 diabetes (cases) and autoantibody-negative controls included in the ATAC-seq/RNA-seq experiments. Values are *N* (%) or mean ± SD as indicated.

PBMC, peripheral blood mononuclear cells. *P* values compare cases and controls (sex by Fisher's exact test; age and PBMC viability by Mann–Whitney U test).

Variable	Case	Control	Comparison
Sample size, *N*	12	12	NA
Male sex, *N* (%)	7 (58.3)	8 (66.7)	*P* > 0.9999
Age at visit, mean (years) ± SD	9.8 ± 2.0	12.3 ± 4.0	*P* = 0.096
PBMC viability (%) ± SD	89.0 ± 2.7	88.3 ± 3.5	*P* = 0.350

Tables - Titles and Legends

(Main Table) Table 1 | Demographic and sample characteristics of the paediatric multi-omics cohort.
Data are shown for children with Type 1 diabetes (cases) and autoantibody-negative controls included in

the ATAC-seq/RNA-seq experiments. Values are *N* (%) or mean ± SD as indicated. PBMC, peripheral blood mononuclear cells. *P* values compare cases and controls (sex by Fisher's exact test; age and PBMC viability by Mann–Whitney U test).

Figures

Figure 1

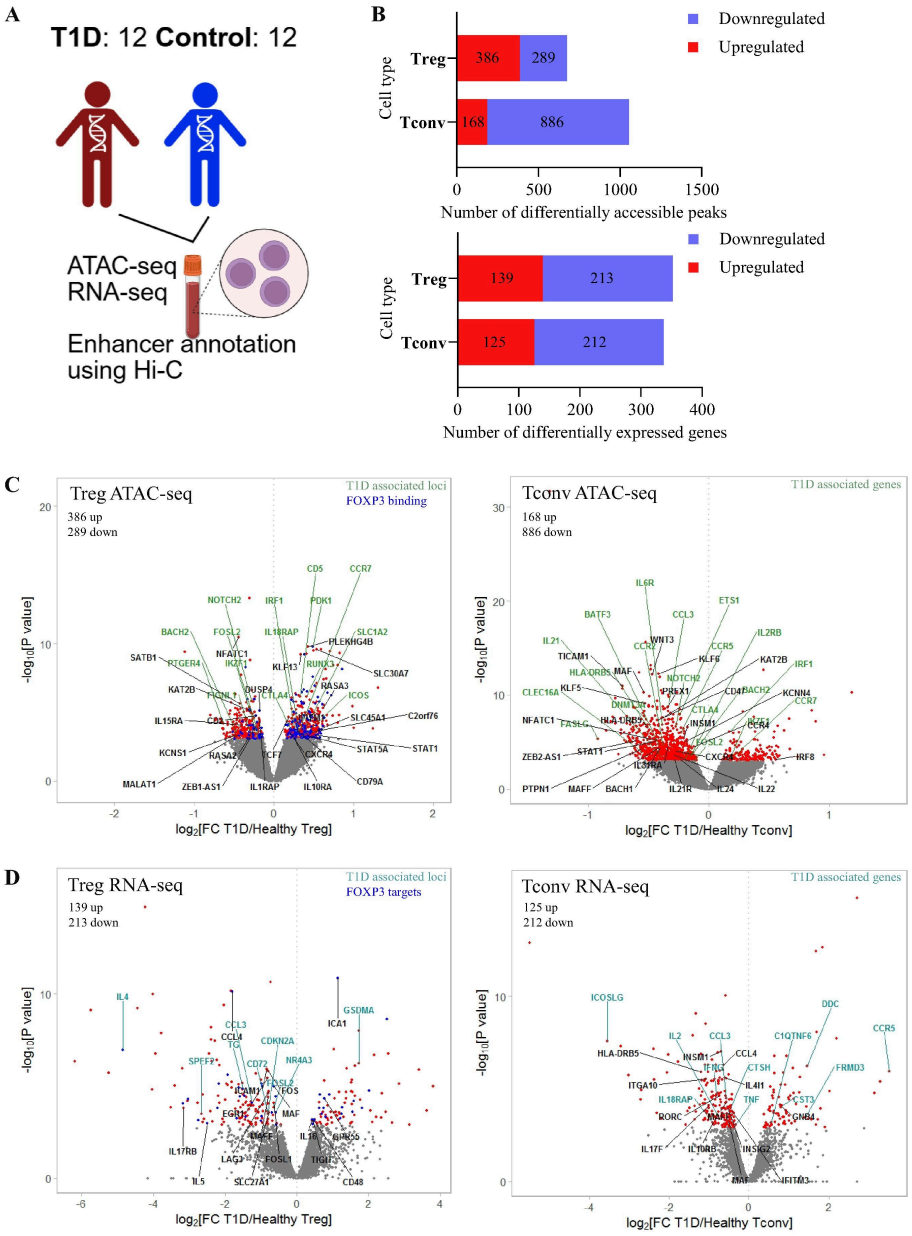


Figure 1

Chromatin accessibility and transcriptional changes in T1D and healthy Treg and Tconv cells.

(A) Study design and multi-omics profiling of T1D and control samples. Peripheral blood samples from 12 individuals with T1D and 12 matched controls were used for integrative epigenomic and transcriptomic profiling. (B) The number of differentially accessible gene loci and expressed genes (Benjamini–Hochberg FDR < 0.05). Up, up-regulated in T1D. Down, down-regulated in T1D. (C–D) Volcano plots comparing normalized chromatin accessibility (C) and expression (D) in Treg and Tconv cells from T1D and healthy control samples. Loci/genes with significant differential accessibility (C) and expression (D) are colored and enumerated. Differential genes previously associated with T1D and/or FOXP3 targets are annotated.

Figure 2

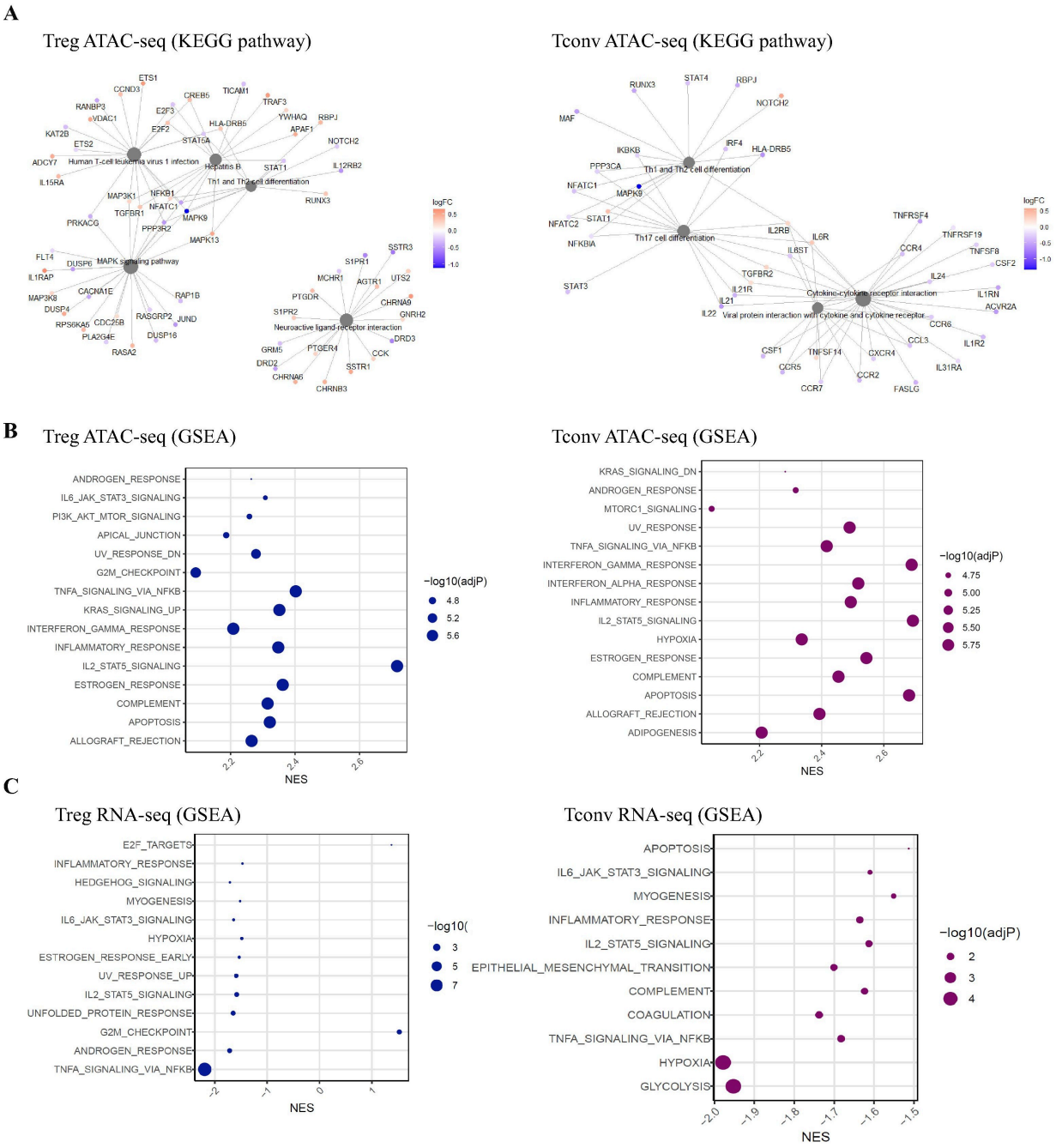


Figure 2

Gene ontology and pathway enrichment showing significantly enriched gene sets between T1D and healthy.

Results from ATAC-seq (A–B) and RNA-seq (C) in Treg and Tconv cells are representative of the combined analysis of 12 and 9 pairs of T1D and sibling-matched healthy control subjects for ATAC-seq

and RNA-seq experiment, respectively. The linkages of genes associated with the enriched pathway or gene ontology terms were demonstrated in the network maps (A and C).

Figure 3

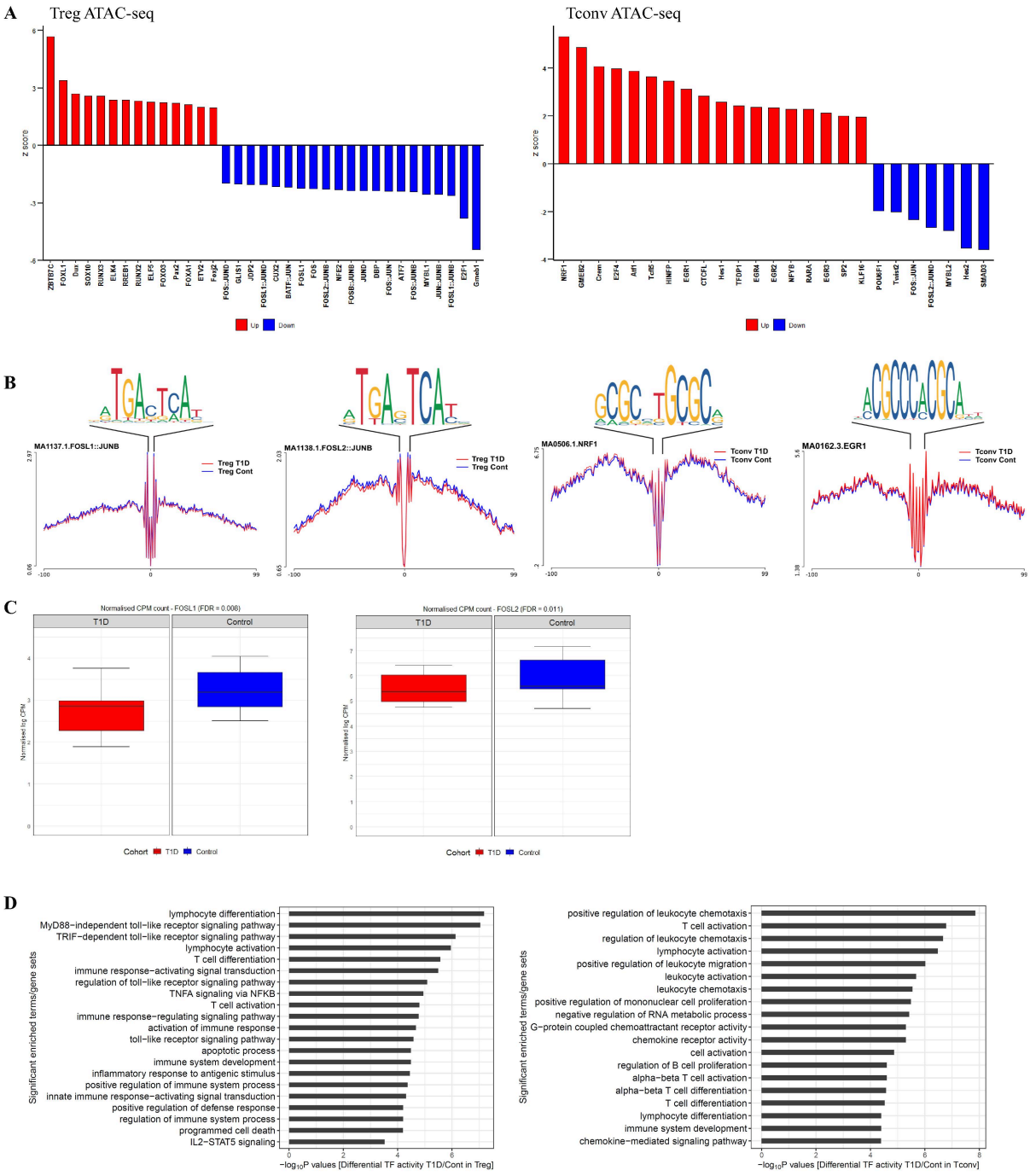


Figure 3

Alterations in transcription factor (TF) dynamics in T cells from T1D patients.

(A) Differential TF footprints within DA ATAC-seq peaks. (B) Representative average ATAC-seq profiles

around selected TF motifs. (C) Expression profiles of corresponding TFs. Higher ATAC-seq signal around the binding motif indicates higher TF activity. (D) Pathway enrichment for genomic regions with differential TF footprints (FDR < 0.05) in Treg and Tconv cells. ATAC-seq signals were computed from pooled data from 12 matched pairs.

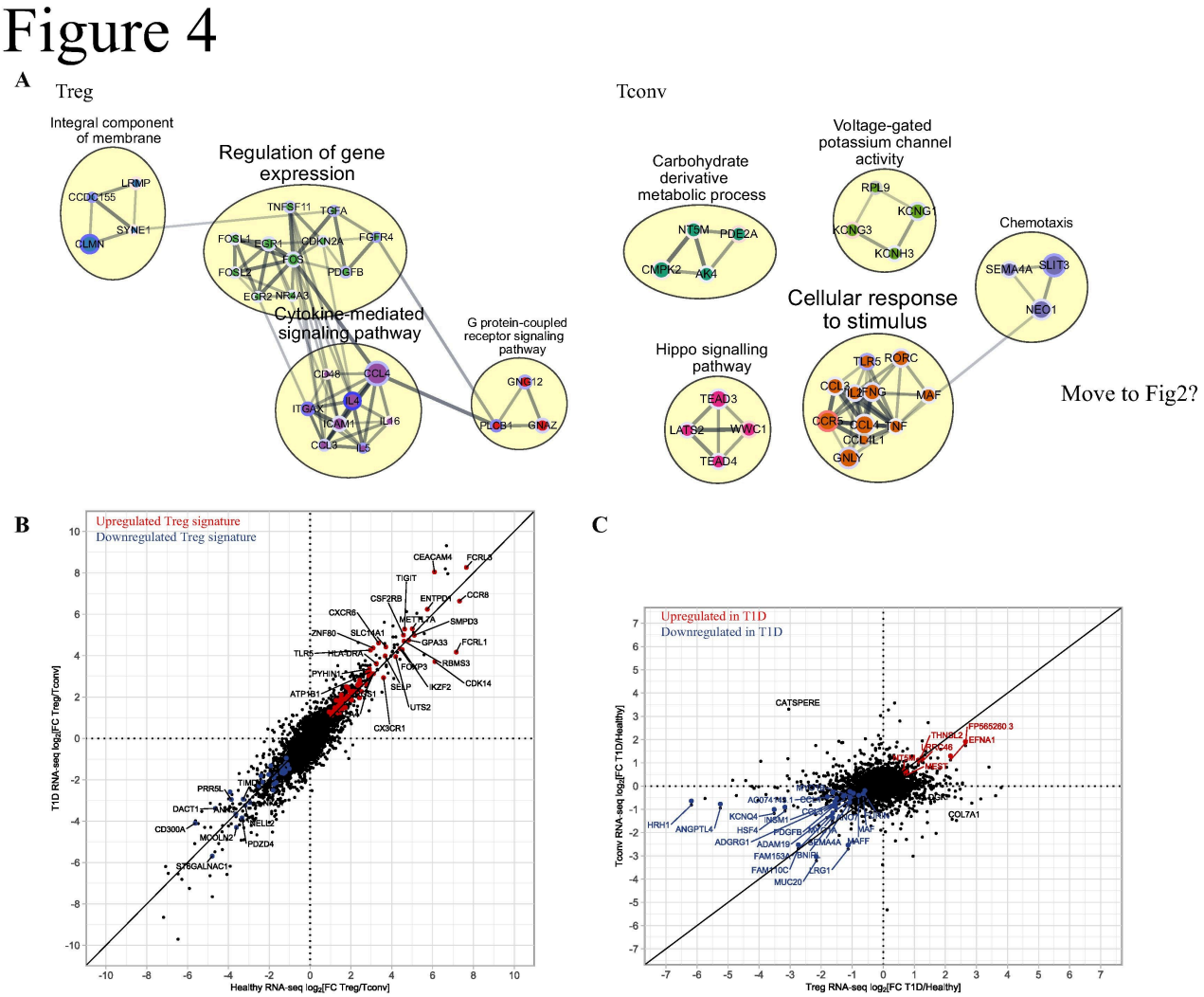


Figure 4

Transcriptional changes in T1D Treg and Tconv cells.
(A) Interaction network of DE genes (FDR < 0.05) between T1D and healthy controls in Treg and Tconv. Node border colour encodes T1D log fold-change; edge colour/thickness reflect interaction confidence (visualized in Cytoscape v3.8.2). (B) Differential expression between Treg and Tconv in T1D and healthy groups; log fold-change in Treg relative to Tconv is shown. Points on the diagonal have the same Treg–Tconv difference in both groups. Points far from the diagonal have a Treg–Tconv contrast that changes between healthy and T1D. Significant genes (FDR < 0.05) that are known Treg signature genes are

annotated. (C) Differential expression for T1D versus healthy in Treg and Tconv compartments. Log fold-change (T1D vs healthy) is shown. Points on the diagonal have the same Treg–Tconv difference in both groups. Points far from the diagonal have a T1D–Control contrast that changes between Treg and Tconv cells. Top 30 common differentially expressed genes in both compartments are annotated.

Figure 5

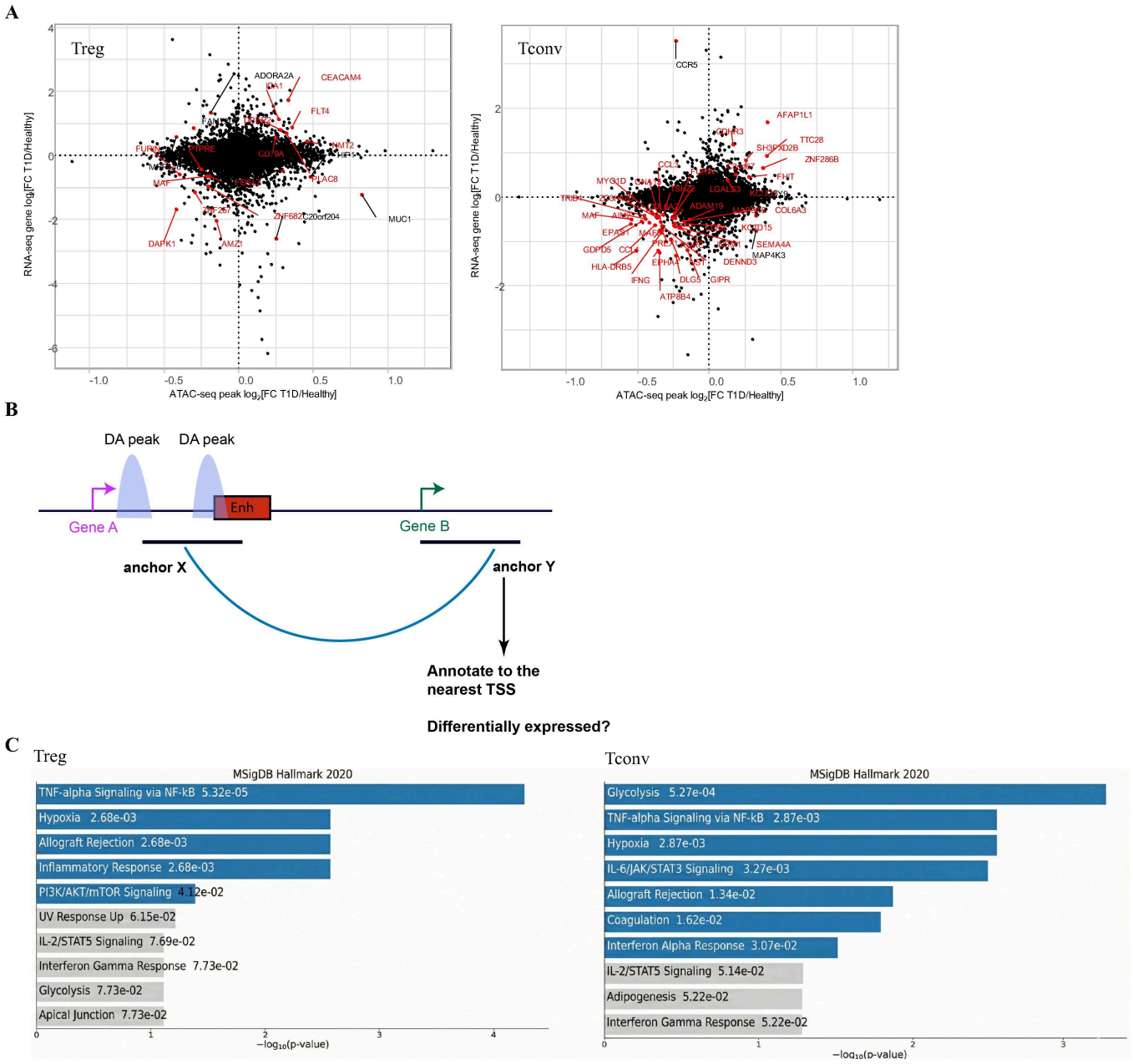


Figure 5

Linking altered enhancers to gene expression and disease pathways using linear and 3D annotation.

(A) Relationship between differential chromatin accessibility and differential gene expression in paediatric Treg (left) and Tconv cells (right) using linear genome annotation. Differential accessibility (DA) analysis was first performed on ATAC-seq peaks (T1D vs control), and DA peaks were then annotated to their nearest gene. For each annotated gene, the x-axis shows the $\log_2$ fold-change in ATAC-seq signal from the DA analysis at its assigned peak(s), and the y-axis shows the $\log_2$ fold-change from the corresponding differential gene expression (DGE) analysis of RNA-seq (T1D vs healthy). Red points mark genes that are significantly differentially accessible/expressed. (B) Schematic illustrating Hi-C–guided reassignment of DA enhancers to distal gene targets. Because enhancers frequently contact promoters that are distant in linear genomic space but juxtaposed in 3D chromatin, annotating DA peaks to the nearest TSS can misassign regulatory targets (Gene A). By integrating public promoter-capture Hi-C maps from human $CD4^+$ T cells with our case–control ATAC-seq data, we instead assign DA enhancers to promoters they contact in 3D (Gene B, anchors X–Y). This strategy identifies long-range enhancer–promoter pairs whose target genes can then be confirmed for differential expression in our case-control Treg and Tconv RNA-seq data. (C) Pathway enrichment for T1D altered genes identified by Hi-C–guided integration of ATAC-seq and RNA-seq in T1D Treg (left) and Tconv cells (right). Bars show selected significantly enriched terms ($-\log_{10}$ *P*value) for the set of genes that are both connected to DA enhancers by promoter-capture Hi-C and differentially expressed in T1D versus controls.

Figure 6

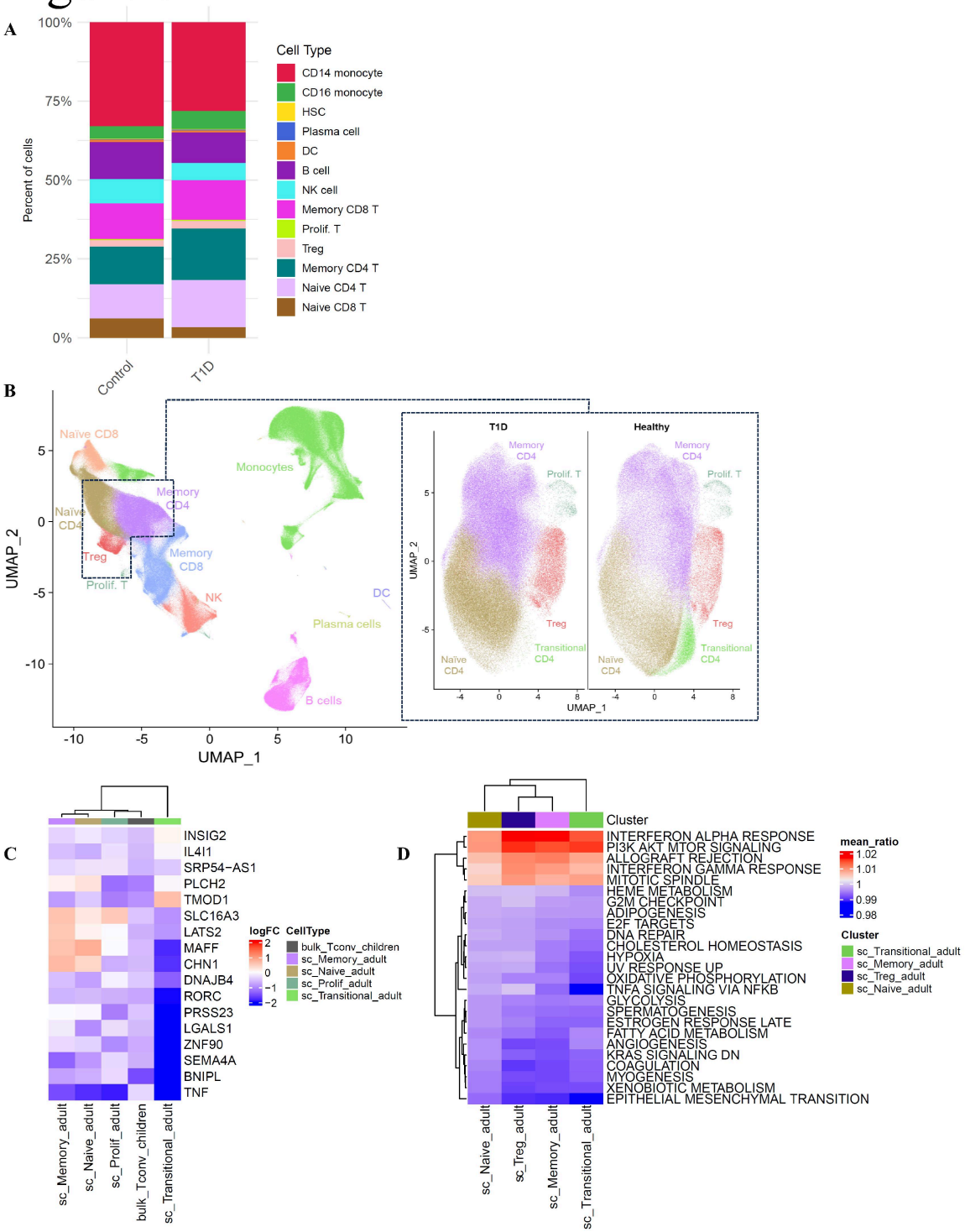


Figure 6

Significant overlap between adult T1D PBMC single-cell differential gene expression and adolescent bulk CD4 T cell RNA-seq. (A) Stacked bar plots show relative cell-type composition in the public T1D PBMC dataset (Control vs T1D). (B) UMAP of all PBMCs colored by annotated cell types (Naive/Memory CD4 and CD8, Treg, Proliferating T, NK, B, Plasma, DCs, CD14/CD16 monocytes, HSCs) with condition-split UMAPs zooming to CD4 subsets. (C) Heatmap of selected genes showing cross-modality

agreement between single-cell CD4 subsets (adult PBMCs) and our adolescent bulk Tconv RNA-seq. Colours denote log2 fold-change (T1D vs control) per cell type. (D) Hierarchically clustered heatmap showing pathway activity (MSigDB Hallmark gene sets) across CD4 T-cell clusters from the public adult T1D PBMC single-cell dataset used in this study. Columns are clusters and rows are pathways. Colours denote the mean, cluster-level enrichment score (centered and scaled per pathway; red = higher, blue = lower; scale at right). Dendrograms indicate hierarchical clustering of clusters and pathways.

Figure 7

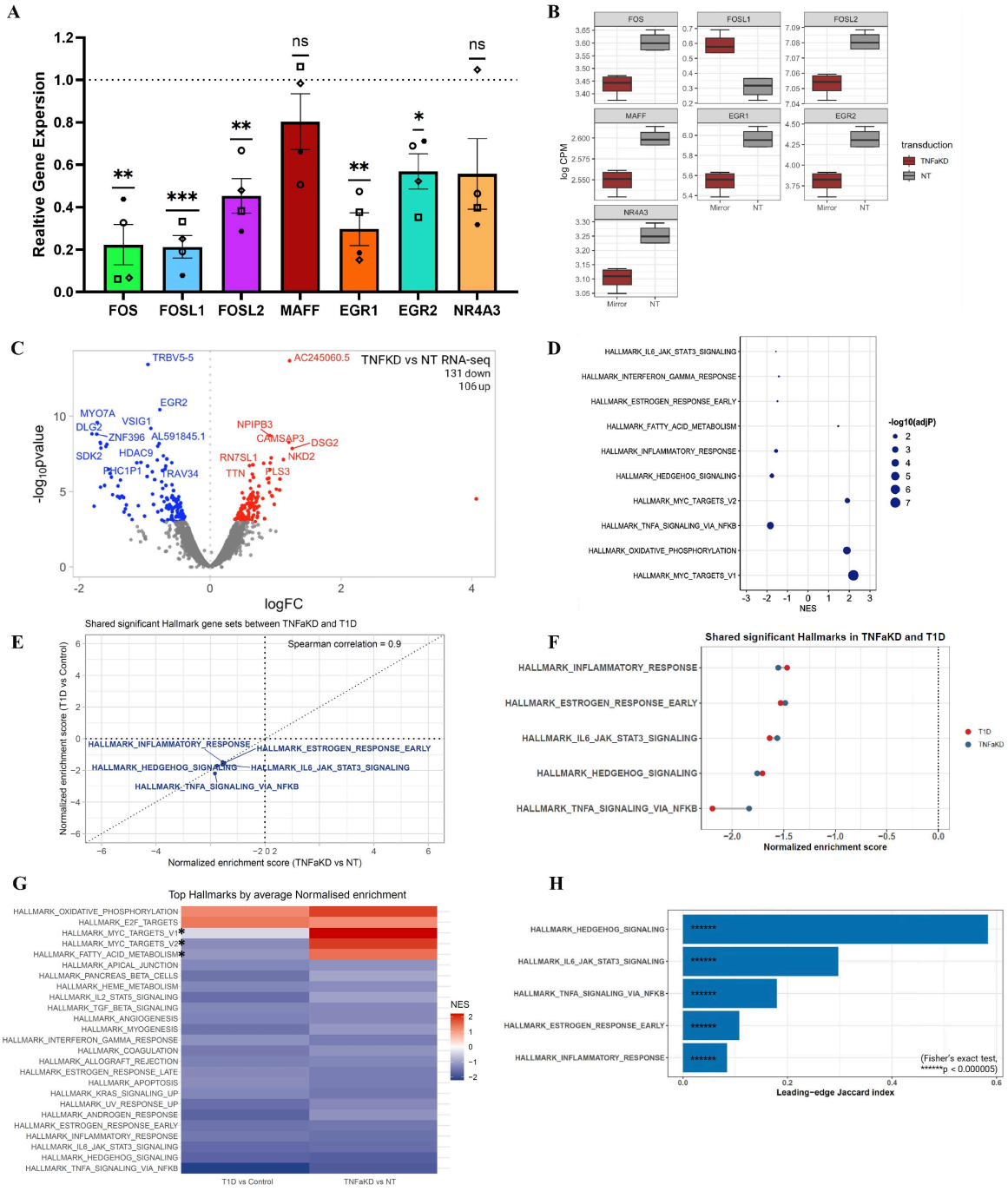


Figure 7

MEGA CRISPR–RfxCas13d knockdown of TNFα/NF-κB seven-TF module.

(A) Relative gene expression from cells transduced with KD-targeting guide virus normalised to the NT control of each donor (n = 4, one sample t-test comparing to a theoretical mean of 1.0). (B) Log2CPM for the 7 MEGA transcription factors in cells transduced with the KD-targeting (red), and NT (grey) arrays after normalisation (Error bards show 1 SD, n = 4 paired donors ****p < 0.0005, ******p < 0.000005). (C) Volcano plot from the TNFαKD compared to their NT controls. The top 30 DE genes are labeled, red dots represent upregulated genes, and blue downregulate (FDR of 0.05, n = 4 paired donors). (D) GSEA (hallmark pathways) of TNFαKD and their NT controls, after normalisation (FDR of 0.1, n = 4 paired donors). (E) Correlation plot of the 5 GSEA hallmark pathways common to the TNFαKD and TIGs T1D patient data (Spearman correlation p = 0.037, Binomial direction test p = 0.0312). (F) Common GSEA hallmark pathways between the TNFαKD group (blue) and T1D patient data (red), showing close concordance between datasets (FDR of 0.1 for the KD-targeting, n = 4 paired donors; FDR of 0.05 for the TIGs data, n = 12 donors). (G) Heatmap of all GSEA hallmark pathways enriched in TNFαKD group and T1D patient data. There is a high agreement in direction of most pathways, but those showing a significant difference are marked with * (FDR of 0.1 for the KD-targeting, n = 4 paired donors; FDR of 0.05 for the TIGs data, n = 12 donors). (H) Jaccard index for the similarly of leading-edge gene driving the 5 GSEA hallmark pathways common to the KD-targeting group and TIGs patient data, and the likelihood that the overlap of each pathway is by random chance (Fisher's exact test, ******p < 0.000005).

Supplementary Files

This is a list of supplementary files associated with this preprint. Click to download.

- Additionalfile.docx
- fig1.jpg